Switching Behavior of Single Nanowires Inside Dense Nickel Nanowire Arrays

K. Nielsch, R. Hertel, R. B. Wehrspohn, J. Barthel, J. Kirschner, U. Gösele, S. F. Fischer, and H. Kronmüller

***Abstract*—We report on the micromagnetic properties of highly regular hexagonal arrays of Ni nanowires, fabricated by means of electodeposition in self-ordered porous alumina. Arrays with interpore distances of 65 and 100 nm and pore diameters of 25 and 30 nm are investigated. From hysteresis loops obtained from measurements with a superconducting quantum interference device (SQUID) magnetometer, the switching field H_{sw} of the nanowires and its deviation ΔH_{sw} is derived. Dynamic micromagnetic modeling using the finite-element method is applied to study the reversal process in an external field. It is shown that starting at the wires' ends, the reversal occurs by means of 180° head-on domain walls propagating along the wire.**

***Index Terms*—Electrodeposition, micro-magnetic modeling, nanowire array, patterned media, porous alumina.**

I. Introduction

THE possibility to obtain tailored nanostructured magnetic materials has stimulated a world-wide research effort toward innovative products in the fields of magnetic storage, bio-medical diagnostics, and drug delivery. Patterned perpendicular storage media consisting of magnetic nanowire arrays [1]–[4] in an magnetically insulating matrix allow high storage densities [5]. More than 700 Gbit/in^2 areal density has been predicted for these structures. Furthermore, these nanowire arrays are very well suited for the preparation of ferrofluidic solutions containing monodisperse nanowires, which are very promising for effective cancer treatments and diagnostic methods [6]. One promising technique to obtain highly ordered magnetic nanowire arrays is based on hexagonally arranged porous-alumina templates [5], [7]–[9].

Since 1981, there have been numerous studies on ferromagnetic nanowire arrays in disordered alumina templates [5], [7], [8]. These structures had large size distributions of the pore diameter and interpore distance, and the filling degree of the pores was not specified. Based on a recent approach by Masuda [10], ordered alumina pore channel arrays can be obtained with a sharply defined pore diameter (<10%) [11], [12]. The degree of self-ordering is polydomain with a typical domain size of a few microns, i.e., more than 20 times the interpore distance. The nearly perfect pore arrangement occurs for interpore distances of $D_{\mathrm{Int}} = 65$ and 100 nm with adjustable pore diameters from $D_P = 25$ to 70 nm.

Here, we will focus on nickel as a filling material due to its negligible magneto-crystalline anisotropy so that the interactions between the anisotropy resulting from the nanowire shape and the stray field inside the magnetic arrays can be studied in detail. The small magnetic moment of Ni, compared with Fe and Co, leads to low dipole interactions between nanowires [2].

Manuscript received February 14, 2002.

K. Nielsch, R. Hertel, R. B. Wehrspohn, J. Barthel, J. Kirschner and U. Gösele are with Max-Planck-Institute of Microstructure Physics, Halle, Germany (e-mail: elch@mpi-halle.de).

S. F. Fischer is with Department of Electronic Materials, Ruhr University Bochum, Bochum, Germany.

H. Kronmüller is with Max-Planck-Institute of Metal Research, Stuttgart, Germany.

Digital Object Identifier 10.1109/TMAG.2002.801955.

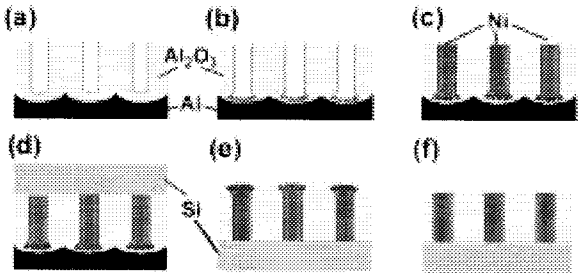

Fig. 1. Preparation steps for fabrication of highly ordered nickel nanowire arrays embedded in an alumina matrix and fixed to a Si substrate (see text).

II. Sample Preparation

Hexagonally-ordered porous Al_2O_3 templates were first fabricated on aluminum substrates using a two-step electrochemical anodization process [10], [13] [see Fig. 1(a)]. The formation of small dendrite pores at the pore bottom promotes a homogeneous nucleation for the electrochemical deposition inside the pores [see Fig. 1(b)] [13]. Nickel was directly plated onto the nearly insulating barrier oxide at the pore bottom from a Watts-type electrolyte and by current pulses [see Fig. 1(c)]. This technique yields a homogeneous Ni filling of the high aspect-ratio pore channels [13]. Subsequently, Si substrates were fixed on top of the array [see Fig. 1(d)], the Al substrate was selectively removed by chemical etching, and the sample was turned upside down [see Fig. 1(e)]. In order to reduce the stray field interactions between the nanowires, the barrier layer and the dendrite part of the nanowires were removed by sputtering with a focused ion beam [see Fig. 1(e)]. Scanning electron micrographs (see Fig. 2) of the nanowire structures revealed a wire length of about 700 nm, column spacing of $D_{\mathrm{Int}} = 100$ nm, and a column diameter of $D_P \approx 30$ nm. Samples with $D_{\mathrm{Int}} = 65$ nm and $D_P = 25$ nm were also obtained.

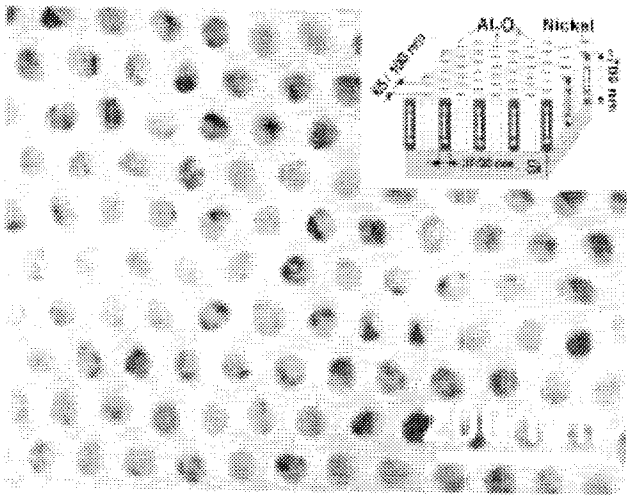

Fig. 2. TEM micrograph of a nickel-filled alumina matrix with an interwire distance of 65 nm. The Ni columns have a diameter of 25 nm.

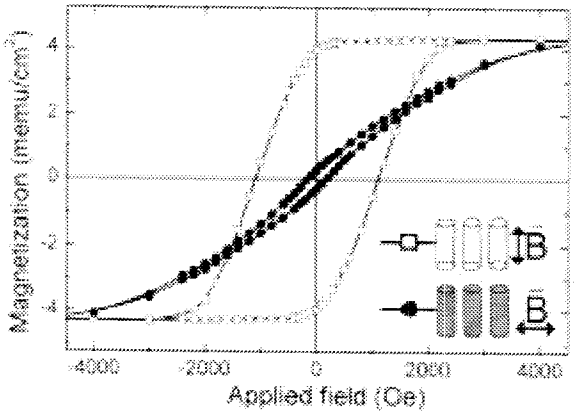

Fig. 3. SQUID-hysteresis loops of the Ni nanowire array with a periodicity of $D_{\rm Int} = 65$ nm and a column diameter of $D_P = 25$ nm.

III. Results and Discussion

For the characterization of the bulk-magnetic properties, a superconducting quantum interference device (SQUID) magnetometer was used. Fig. 3 shows the hysteresis loop for the sample with $D_{\rm Int} = 65$ nm and $D_P = 25$ nm. The measured hysteresis for an applied field parallel to the axis of the nanowires exhibit a coercivity $H_c^{\parallel} \approx 1100$ Oe and a squareness close to 100%. This sample has its preferential magnetic orientation along the column axis. In the perpendicular direction, the coercivity is small ($H_c^{\perp} \approx 150$ Oe), large magnetic fields are required for a complete magnetization, and the loop shows a nearly reversible behavior. As shown recently, for this arrangement, each Ni nanowire is a single domain particle, and its anisotropy is determined by the particle shape [8]. When this magnetic array is completely magnetized in the preferential magnetic orientation, the average internal stray field between the nanowires is $H_D^{\parallel} = 2\pi^{3/2}(D_P/D_{\rm Int})^2 \cdot M_S = 770$ Oe [8] and, thus, smaller than $H_c^{\parallel}$. Each Ni nanowire has on average a switching field $H_{\rm sw} \approx H_c^{\parallel}$ with a standard deviation $\Delta H_{\rm sw}$, due to the diameter variation. After the sample has been saturated along the nanowire axis and the magnetic field has been switched off, a very small fraction of nanowires reverse their magnetization because locally, $(H_{\rm sw} - \Delta H_{\rm sw}) < H_D$. This explains the small deviation of the measured squareness (96%) from the expected value of 100% for $H_D^{\parallel} < H_C^{\parallel}$.

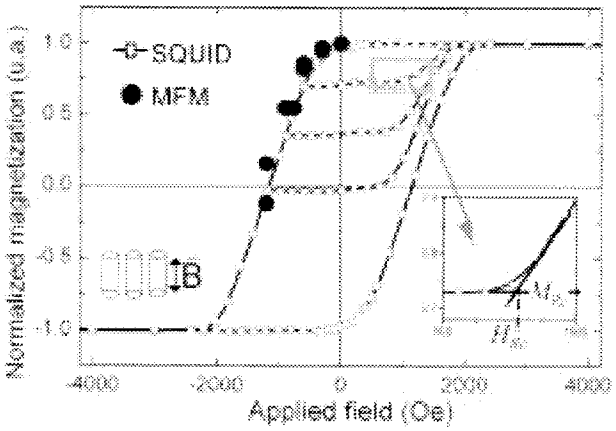

Fig. 4. Major hysteresis loop and recoil loops of a Ni nanowire array with $D_{\rm Int} = 100$ nm and $D_P = 30$. The results of statistically analyzed MFM images are compared with the experimental hysteresis loops.

For a decrease in $(D_P/D_{\rm Int})$, the dipolar interactions inside the array will be reduced. Fig. 4 shows the major hysteresis loop for the sample with $D_{\rm Int} = 100$ nm and $D_P = 30$ nm, which exhibits a slightly enhanced coercivity ($H_c^{\parallel} \approx 1200$ Oe) and squareness (100%). Due to the reduction of $D_P/D_{\rm Int} = 0.39 \rightarrow 0.3$, this sample has a lower demagntization field of $H_D^{\parallel} = 455$ Oe as compared with Fig. 2. This value is considerably lower than $H_{\rm sw}$ of the magnetically weakest nanowires inside the array. Therefore, no nanowire should reverse its magnetic polarization after the sample has been completely magnetized. This has also been observed recently by magnetic force microcopy (MFM) [14]. The statistical results from the analyses of MFM images, measured in the presence of an external magnetic field, are also plotted in Fig. 4 and are in good agreement with the SQUID results.

In order to estimate the switching field distribution $\Delta H_{\rm sw}$, we have recorded a number of recoil hysteresis loops (see Fig. 4). Each curve has a nearly steady magnetization $M_{\rm Rc}$ below its switching field $H_{\rm Rc}$ (see the inset of Fig. 4). For each $H_{\rm Rc}$, the effective average field inside the magnetic arrays was calculated: $H_{\rm eff,Rc} = H_{\rm Rc} - H_D^{\parallel} \cdot M_{\rm Rc}/M_S$. Subsequently, the effective magnetization of each recoil hysteresis $M_{\rm eff,Rc} = 1 - M_{\rm Rc}/M_S$ has been plotted as a function of $H_{\rm eff,Rc}$. By fitting these data to the integral function of the Gaussian standard distribution, we obtained $\Delta H_{\rm sw} = 180$ Oe. $\Delta H_{\rm sw}$ is about 15% of H_C for a distribution $\Delta D_P/D_P$ of 8%. Both values are in good aggreementv if we assume that $H_{\rm sw}$ of a single nanowire is proportional to $1/D_P^2$. This value is significant for the simulation of the major hysteresis loops of a nanomagnet array, as shown by Ross *et al.* [15].

IV. Micromagnetic Modeling

The influence of the magnetostatic interactions on the coercive field in a set of nanowires has been investigated

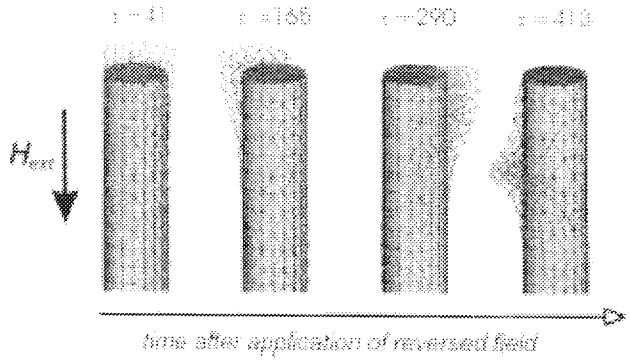

Fig. 5. Initial stages of the reversal process in a Ni wire with 25 nm diameter, exposed to an external field of 150 mT. The reduced (dimensionless) time scale $\tau = t\gamma M_s$ is used. A Gilbert damping parameter $\alpha = 0.1$ is assumed.

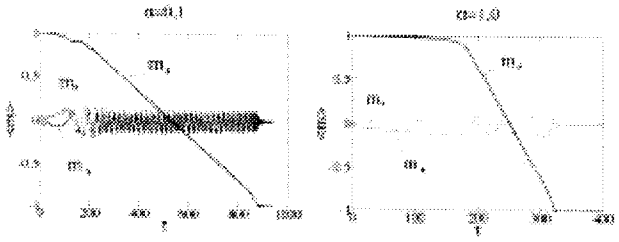

Fig. 6. Average magnetization components in a 25 nm wire as a function of time during the switching process for $\alpha = 0.1$ and $\alpha = 1.0$. The wire axis is along z.

recently by means of micromagnetic simulations based on energy minimization [17]. In order to study the reversal process of a single wire, time-resolved micromagnetic modeling is required. Gilbert's equation

$$\frac{d}{dt}\vec{M} = -\gamma\left(\vec{M} \times \vec{H}_{\text{eff}}\right) + \frac{\alpha}{M_s}\left(\vec{M} \times \frac{d\vec{M}}{dt}\right) \qquad (1)$$

describes the temporal evolution of the magnetization $\boldsymbol{M}$, where the effective field $\mathbf{H}_{\text{eff}}$ is derived from the micromagnetic energy density e according to $\mathbf{H}_{\text{eff}} = -\delta e/\delta \boldsymbol{m}$. The stray field is calculated by means of a hybrid finite-element/boundary-element method [17]. An important feature of the finite element method is that it allows for good geometrical approximations of particles with curved boundaries (see the mesh in Fig. 5) [18]. The reversal of two Ni wires has been simulated: one with 30 nm and one with 25 nm diameter, both of 700 nm length. A field of 150 mT is applied instantaneoulsy, nominally antiparallel to the magnetization. The sudden exposure to the magnetic field does not cause an immediate response of the magnetization, which indicates that this step-like application of the field is a good model for the switching process, regardless of the exact slope of the external field in time. The reversal starts at the wire's ends. Two 180° head-on domain walls nucleate, at the top and at the bottom of the wire, which propagate through the wire, thus expanding the reversed domains (see Fig. 5). In the middle of the head-on walls, the magnetization points perpendicular to the wire axis. The external field exerts a strong torque on the magnetization in these regions so that the magnetic moments precess around the wire. This shows up in oscillations of the average magnetization components perpendicular to the wire axis. For both wires, the reversal mechanism is the same so that only one example is reported in Fig. 6. A different reversal by means of a localized curling mode has been reported recently for Ni nanowires with larger diameter (60 nm) [19]. In the wires we investigated, the reversal mode does not depend on the damping parameter α, which, however, determines the speed of the switching process. For low values of α, the domain wall propagates slowly, and numerous precession cycles occur, whereas high damping leads to a fast magnetization reversal.

REFERENCES

[1] S. Y. Chou, M. S. Wei, P. R. Krauss, and P. B. Fischer, "Single-domain magnetic pillar array for ultrahigh density quantum magnetic storage," *J. Appl. Phys.*, vol. 76, pp. 6673–75, 1994.

[2] C. A. Ross, H. I. Smith, T. A. Savas, M. Schattenberg, M. Farhoud, M. Hwang, M. Walsh, M. C. Abraham, and R. J. Ram, "Fabrication of patterned media for high density magnetic storage," *J. Vac. Sci. Technol.*, vol. B17, pp. 3168–76, 1999.

[3] T. Thurn-Albrecht, J. Schotter, C. A. Kastle, N. Emley, T. Shibauchi, L. Krusin-Elbaum, K. Guarini, C. T. Black, M. T. Tuominen, and T. P. Russell, "Ultrahigh-density nanowire arrays grown in self-assembled diblock copolymer templates," *Sci.*, vol. 290, pp. 2126–29, 2000.

[4] M. Zenger, W. Breuer, M. Zölfl, R. Pulwey, J. Raabe, and D. Weiss, "Electrodeposition of NiFe and Fe nanopillars," *IEEE Trans. Magn.*, vol. 37, pp. 2094–2096, July 2001.

[5] S. Kawai and R. Ueda, "Magnetic properties of anodic oxide coating on aluminum containing electrodeposited Co and Co-Ni," *J. Electrochem. Soc.*, vol. 122, pp. 32–36, 1975.

[6] H. Schmidt, "Nanoparticles by chemical synthesis, processing to materials and innovative applications," *Appl. Organometr. Chem.*, vol. 15, pp. 331–343, 2001.

[7] D. AlMawlawi, N. Coombs, and M. Moskovits, "Magnetic properties of Fe deposited into anodic aluminum oxide pores as a function of particle size," *J. Appl. Phys.*, vol. 69, pp. 5150–52, 1991.

[8] J. Sellmyer, M. Zheng, and R. Skomski, "Magnetic properties of self-assembled Co nanowires of varying length and diameter," *J. Phys. Condens. Matter.*, vol. 13, pp. R433–480, 2001.

[9] K. Nielsch, R. B. Wehrspohn, J. Barthel, J. Kirschner, U. Gösele, S. F. Fischer, and H. Kronmüller, "Hexagonally ordered 100 nm period Nickel nanowire arrays," *Appl. Phys. Lett.*, vol. 79, pp. 1360–62, 2001.

[10] H. Masuda and K. Fukuda, "Ordered metal nanohole arrays by a two-step replication of honeycombstructures of anodic alumina," *Sci.*, vol. 268, pp. 1466–69, 1995.

[11] O. Jessensky, F. Müller, and U. Gösele, "Self-organized formation of hexagonal pore arrays in anodic alumina," *Appl. Phys. Lett.*, vol. 72, pp. 1173–75, 1998.

[12] A. P. Li, F. Müller, A. Birner, K. Nielsch, and U. Gösele, "Hexagonal pore arrays with 50–420 nm interpore distance formed by self organization in anodic alumina," *J. Appl. Phys.*, vol. 84, pp. 6023–26, 1999.

[13] K. Nielsch, F. Müller, A. P. Li, and U. Gösele, "Uniform Nickel deposition into ordered alumina pores by pulsed electrodeposition," *Adv. Mater.*, vol. 12, pp. 582–586, 2000.

[14] K. Nielsch, R. B. Wehrspohn, J. Barthel, J. Kirschner, S. F. Fischer, H. Kronmüller, T. Schweinböck, D. Weiss, and U. G. Gösele, "High density hexagonal Nickel nanowire array," *J. Magn. Magn. Mater.*, July 2002, to be published.

[15] M. Hwang, M. Farhoud, Y. Hao, M. Walsh, T. A. Savas, H. I. Smith, and C. A. Ross, "Major hysteresis loop modeling of two-dimensional arrays of single domain particles," *IEEE Trans. Magn.*, vol. 36, pp. 3173–3175, Sept. 2000.

[16] R. Hertel, "Micromagnetic simulations of magnetostatically coupled Nickel nanowires," *J. Appl. Phys.*, vol. 90, pp. 5752–58, 2001.

[17] D. R. Fredkin and T. R. Koehler, "Hybrid method for computing demagnetized fields," *IEEE Trans. Magn.*, vol. 26, pp. 415–417, Mar. 1990.

[18] C. J. Garcia-Cervera, Z. Gimbutas, and E. Weinan, "Accurate numerical methods for micromagnetics simulations with general geometries," J. Comput. Phys, 2001, submitted for publication.

[19] R. Hertel, "Computational micromagnetism of magnetization processes in Nickel nanowires," *J. Magn. Magn. Mater.*, July 2002, to be published.